Geofísica Internacional (2007), Vol. 46, Num. 1, pp. 3-18

The seismic and hydroacoustic stations on Socorro Island: Early results

Raúl W. Valenzuela[1], Javier F. Pacheco[1], José Pereira[2], Jorge A. Estrada[3], Jesús A. Pérez[3], José L. Cruz[3], Dario Baturan[4], Arturo Cárdenas[3] and José A. Santiago[3]

[1] *Departamento de Sismología, Instituto de Geofísica, UNAM, Mexico City, Mexico*
[2] *Comprehensive Nuclear-Test-Ban Treaty Organization, IMS, Vienna, Austria*
[3] *Servicio Sismológico Nacional, Instituto de Geofísica, UNAM, Mexico City, Mexico*
[4] *Nanometrics, Inc., Kanata, Ontario, Canada*

Received: November 24, 2005; accepted: December 13, 2006

RESUMEN

El Servicio Sismológico Nacional del Instituto de Geofísica de la Universidad Nacional Autónoma de México y la Organización del Tratado para la Prohibición Completa de Ensayos Nucleares instalaron conjuntamente una red sísmica e hidroacústica en Isla Socorro. En el presente estudio se reporta la detección de diez sismos, ocurridos en junio y julio de 2004. Estos se localizaron a distancias epicentrales entre 209 y 9050 km y sus magnitudes variaron entre 3.9 y 6.8. Se observó la llegada de las ondas *P* y *pP*, telesísmicas y de alta frecuencia, producidas por un evento en la península de Kamchatka a una distancia de 8245 km. Un sismo en la región limítrofe entre Guerrero y Oaxaca generó ondas sísmicas y fases *T* que se aprecian claramente. Se registraron tres sismos en la Zona de Fractura de Rivera, lo cual hace esperar que se seguirán detectando eventos ocurridos en las zonas de fractura cercanas, así como los sismos generados por los volcanes en las Islas Socorro y San Benedicto. El análisis de las fases *T* producidas por varios eventos también permitió validar el diseño de la red, en la cual se emplean tres localidades distintas en la isla para observar el océano en todas direcciones. Las ondas sísmicas de alta frecuencia generadas a partir de las ondas acústicas se atenuan al propagarse en roca desde un extremo al otro de la isla, por lo cual es muy difícil, a veces imposible, detectar eventos pequeños o lejanos en el lado opuesto de la isla.

PALABRAS CLAVE: Tratado para la Prohibición Completa de Ensayos Nucleares (TPCEN), canal de fijación y determinación de la distancia por sonido (SOFAR), explosiones nucleares, Isla Socorro, fases *T*, Zona de Fractura de Rivera, océano Pacífico.

ABSTRACT

A seismic and hydroacoustic network on Socorro Island was installed jointly by the Servicio Sismológico Nacional, Instituto de Geofísica, Universidad Nacional Autónoma de México, and the Comprehensive Nuclear-Test-Ban Treaty Organization. The detection of ten earthquakes in June and July 2004 is reported in this study. These events occurred at epicentral distances between 209 and 9050 km and ranged in magnitude between 3.9 and 6.8. An event in the Kamchatka Peninsula featured arrivals of teleseismic high-frequency *P* and *pP* waves from a distance of 8245 km. An earthquake in the Guerrero-Oaxaca, Mexico, region shows clear seismic and *T* phases. Three earthquakes in the Rivera Fracture Zone were recorded, thus leading to the expectation of the continued detection of events from nearby fracture zones as well as earthquakes generated by volcanoes on Socorro and San Benedicto Islands. The analysis of the *T* phases from several events validates the design of the network, with three sites around the island in order to record arrivals from all directions. High frequency seismic waves generated by acoustic waves attenuate as they propagate through the rock from one end of the island to the other. Consequently small or distant events are difficult to detect at the far side of the island.

KEY WORDS: Comprehensive Nuclear-Test-Ban Treaty (CTBT), Sound Fixing and Ranging (SOFAR) channel, nuclear explosions, Socorro Island, *T* phases, Rivera Fracture Zone, Pacific ocean.

1. INTRODUCTION

The Comprehensive Nuclear-Test-Ban Treaty (CTBT) bans all nuclear explosions, whether for military or civilian purposes. One of the main components of the Comprehensive Nuclear-Test-Ban Treaty Organization (CTBTO) is the International Monitoring System (IMS). The IMS is currently deploying a global network aimed to guarantee compliance with the treaty. This network is built around four different technologies which rely on seismic, hydroacoustic, infrasound, and radionuclide stations (Sullivan, 1998).

The Hydroacoustic Monitoring Section of the IMS is concerned with the detection of acoustic energy from potential nuclear explosions in the oceans. The SOund Fixing And Ranging (SOFAR) channel is a low sound velocity

waveguide in the ocean at depths between 600 and 1800 m (Okal, 2001). It allows for the efficient propagation of high frequency (greater than 2.5 Hz) sound waves (Okal, 2001). CTBTO's hydroacoustic network will be made up of underwater hydrophone stations at six different locations, and island-based *T* phase stations using seismometers at five additional locations around the world (Sullivan, 1998; Newton and Galindo, 2001). These acoustic waves travel through the water at a relatively slow speed, which leads to a good precision for the location of sources based on *T* wave arrival times (Talandier and Okal, 1998). This combination of good detection and location makes *T* waves a useful tool for the monitoring and identification of small sources in remote areas. *T* waves are seismic waves generated when the sound waves traveling through water are transmitted into the rock of an oceanic island or a continent.

Hydroacoustic waves can travel long distances with little attenuation (Talandier and Okal, 1998; Okal, 2001). Therefore, only a few stations is needed to monitor any one of the world's oceans. CTBTO's hydroacoustic network includes only four stations in the Pacific ocean (Sullivan, 1998; Newton and Galindo, 2001). Since Mexico is a signatory of the CTBT, Socorro Island was chosen to provide coverage of the east-central Pacific ocean using seismometers to record *T* waves. The Servicio Sismológico Nacional (SSN) at the Instituto de Geofísica of the Universidad Nacional Autónoma de México, the Mexican National University, jointly with the IMS, operates the *T* phase station in Socorro Island. In order to provide good coverage of the ocean in all directions, it became necessary to deploy seismometers at three different locations around the island. Under the IMS convention, the term "station" describes the seismometers installed at the three different sites. In this study, however, the term "network" will describe the three locations at the island collectively, while the term "station" will be applied individually to any one of the various sites.

In June 1999, a site survey was conducted jointly by SSN and CTBTO at Socorro Island in order to determine the design for its hydroacoustic network (Valenzuela *et al*., 2005). During that first trip, only sites in the southeastern corner of the island were occupied. As a result of the survey, site SRAD (Table 1, Figure 1; Valenzuela *et al*., 2005) was chosen to build one of the stations because this site could detect *T* waves coming from the northeast, the east and the southeast. Due to the size of the island and to the rapid attenuation of high frequency signals traveling through rock, it was hard to detect the *T* phases from events in the northwest, the west and the southwest. During a second survey conducted in February 2002, two additional sites SPLN and SPEL (Table 1, Figure 1) were chosen (R. W. Valenzuela, unpublished, 2003). Construction at all three sites started in December 2003 and was concluded in May 2004. The equipment was installed in May 2004. We describe the characteristics of the stations and the observations from the first weeks of operation. Seismic and/or hydroacoustic signals produced by ten earthquakes recorded through early July 2004 are presented in this study. These events occurred at distances between 209 and 9050 km and ranged in magnitude from 3.9 to 6.8. *T* waves produced by events at five different locations around the Pacific were also recorded.

2. DESCRIPTION OF THE STATIONS

Socorro Island belongs to the Revillagigedo Archipelago located at approximately 18.8° N, 111.0° W in the eastern Pacific ocean (Figure 1). The island has an elongated NW-SE shape with maximum dimensions of about 15 km × 15 km in the N-S and E-W directions. The Mexican port of Manzanillo, Colima, is about 700 km east from the island. Socorro is the emergent peak of a large basaltic shield volcano that rises from the sea floor at a depth of ~3000 m. Its highest elevation is Mount Evermann at 1050 m above mean sea level. The island's average submarine slope is a little less than 10° (Siebe *et al*., 1995).

The three sites on the island were chosen to provide good azimuthal coverage so that *T* phases can be detected from any direction in the Pacific ocean. Table 1 lists the locations and codes for the stations; also see Figure 1. Station SRAD is the eastern site of the array. It is built near the ruined building of a small radar station formerly used for the island's landing strip. SPEL is at the south side of the island, near the shoreline and close to a small hill. It is close to the Navy settlement of the island. The third site, SPLN, is located at the northernmost tip of the island. It can only be reached by boat. People can land on a beach (Playa Norte) and walk to the station, which is part way up a small hill.

The three stations have essentially the same design and equipment. Figure 2 shows the SRAD site. There are two small buildings at each site. One of them houses the seismometers and is partly buried in the ground. The roof stands 1.5 m above the ground surface. Access is through a roof scuttle. The floor is located about 1 m below the ground surface. The seismometers were placed over a concrete pad which is about 0.5 m below the floor surface (Figure 3). The second building is a shed housing batteries and electric equipment. A VSAT dish antenna is used for satellite communication to the Central Recording Facility at the SSN office in Mexico City. Data are stored at SSN on a Sun workstation computer and are copied to Vienna via satellite. A solar panel is mounted on the roof of the shed and a wind generator is also used to charge the batteries running the equipment. Lightning protection is provided from an Erico Dynasphere device mounted on an aluminum mast. The buildings and other equipment are grounded. Since *T* waves have high frequencies, short period GS-13 seismometers are used. There are three seismometers at each site, one vertical and north-south and east-west horizontals (Figure 3). Station

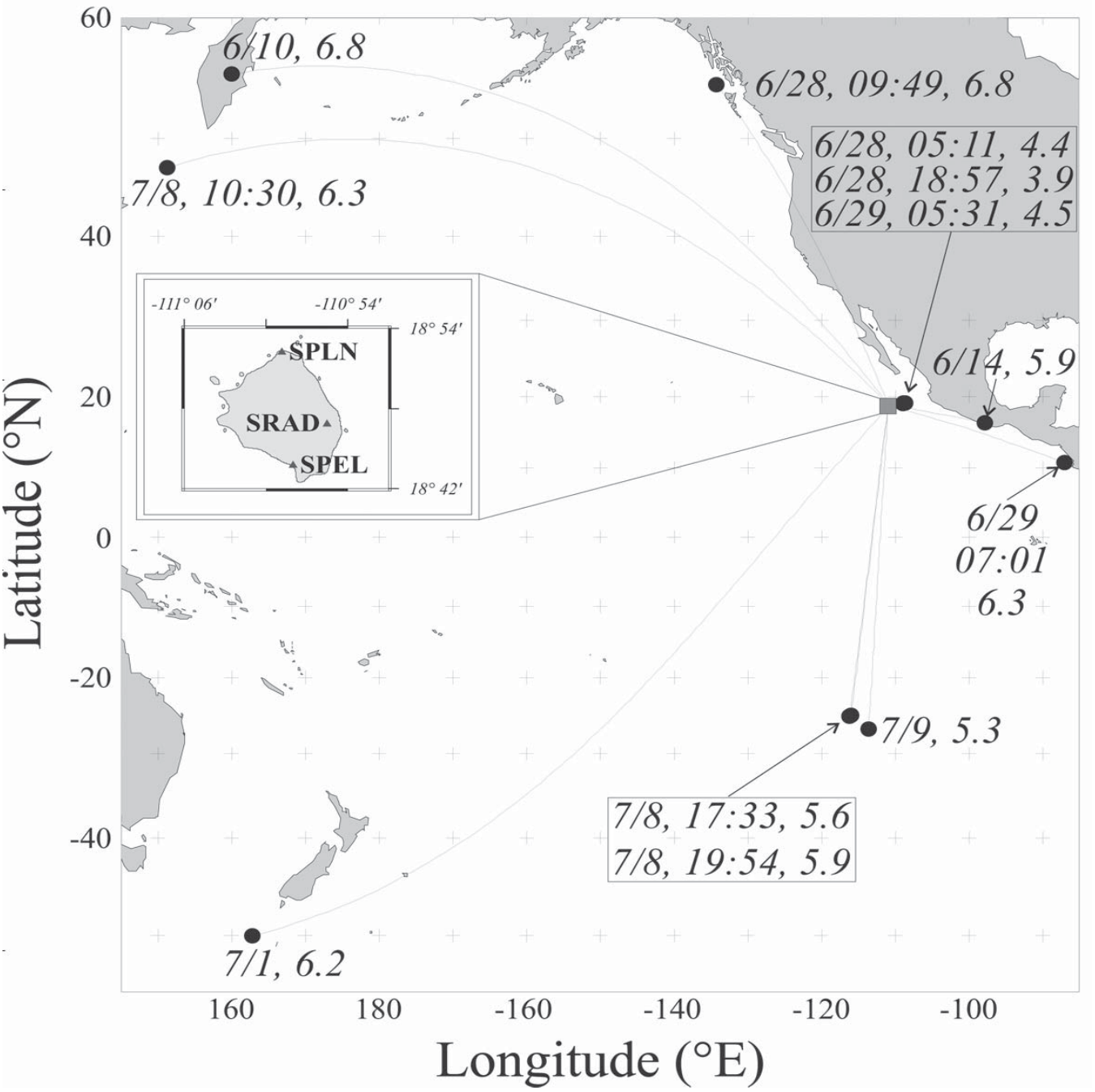

Fig. 1. Location map of Socorro Island and location of the earthquakes reported in this study together with their great circle paths. The triangles in the inset show the location of the three stations on the island. The dots mark the epicenters of events in June and July 2004. The first number associated with each earthquake is the date. If more than one event was recorded on the same day, the origin time is given in hours and minutes. The last number is the magnitude.

SRAD has a Streckeisen STS-2 broadband, three-component seismometer. Nanometrics Europa digitizers are used at all three sites. The GS-13 seismometer has a corner frequency of 1 Hz and a flat velocity response at higher frequencies. The corner frequency for the STS-2 seismometer is at 120 s (0.00833 Hz) and the velocity response is flat at higher frequencies. The velocity response is flat for both the GS-13 and the STS-2 up to 50 Hz.

3. SEISMIC PHASES RECORDED AT SOCORRO ISLAND

During the period from June 10 to July 9, 2004 twelve earthquakes were singled out for analysis because of their location and magnitude. These events were identified from the Preliminary Determination of Epicenters (PDE) listing produced by the United States Geological Survey

Fig. 2. Picture of station SRAD (H06E1) located near the landing strip and a now destroyed radar station. This is the eastern station of the network. The wind generator, the shed housing electric equipment with a solar panel on top, the lightning protection system, the satellite dish antenna and the seismic vault are shown.

Table 1

Locations of the stations on Socorro Island, May 2004

Station Code	Alternative Code	Seismometer	Latitude	Longitude	Location
SRAD	H06E1	STS-2	18.78° N	110.93° W	Radar station
SPEL	H06S1	GS-13	18.73° N	110.96° W	Barren hill
SPLN	H06N1	GS-13	18.86° N	110.99° W	Northern beach

(USGS). Location within the Pacific Basin was an important consideration. Five of these events have a magnitude greater than or equal to 6.0 and are likely to be recorded at epicentral distances out to 110° (even if they occurred outside of the Pacific Basin). Earthquakes of magnitude greater than or equal to 5.0 were considered if their epicentral distance was 60° or less. Events located on nearby fracture zones or the west coast of Central and North America can be detected at lower magnitudes. For example, the lowest magnitude ($M_c = 3.9$) from this study was for an earthquake on the Rivera

Fracture Zone at an epicentral distance of 2.19° (244 km). We estimate that the detection threshold for local events should be at about M_c = 3.5, although this will require further work to be confirmed. Valenzuela *et al*. (2005) recorded an earthquake at M_c = 2.8 on the Clarion Fracture Zone at an epicentral distance of 42 km. *T* waves are often recorded from events too small to produce detectable *P* and *S* waves at a given distance. Therefore, *T* phases can be useful for the monitoring and identification of small sources in remote areas (Talandier and Okal, 1998). Due to technical problems, only ten of the twelve selected events were actually recorded. Figure 1 shows their epicenters and great circle paths. At the start of this time period all stations were operating; however, data from station SRAD stopped coming after June 29 and station SPEL stopped transmitting on July 9. It was determined that the power supplied to these stations was too low, due to breakdown of the wind generators. Additionally, faulty GPS antennas made it impossible to synchronize the data transmission. These problems were fixed in late January 2005. For these reasons, only three earthquakes were recorded by all three stations. Table 2 summarizes the twelve events giving their date, origin time, hypocenter, magnitude, epicentral distance to station SPLN, number of stations which produced a record, and the geographical location. The parameters presented in Table 2 were taken from several sources and are the most reliable available. These include the National Earthquake Information Center of the United States Geological Survey and Harvard University's Centroid Moment Tensor catalog for global events, and Mexico's Servicio Sismológico Nacional for earthquakes in that country. The locations of three events on the Rivera Fracture Zone were improved using SSN data together with data from the stations on the island. The events recorded have epicentral distances between 209 km (Rivera FZ, to station SRAD; 214 km to SPLN as shown in Table 2) and 9050 km (Kuril Islands). Their magnitudes range from M_c=3.9 (Rivera FZ) to M_w=6.8 (one event in the Kamchatka Peninsula and one in southeastern Alaska). Some observations concerning the different events recorded are presented below.

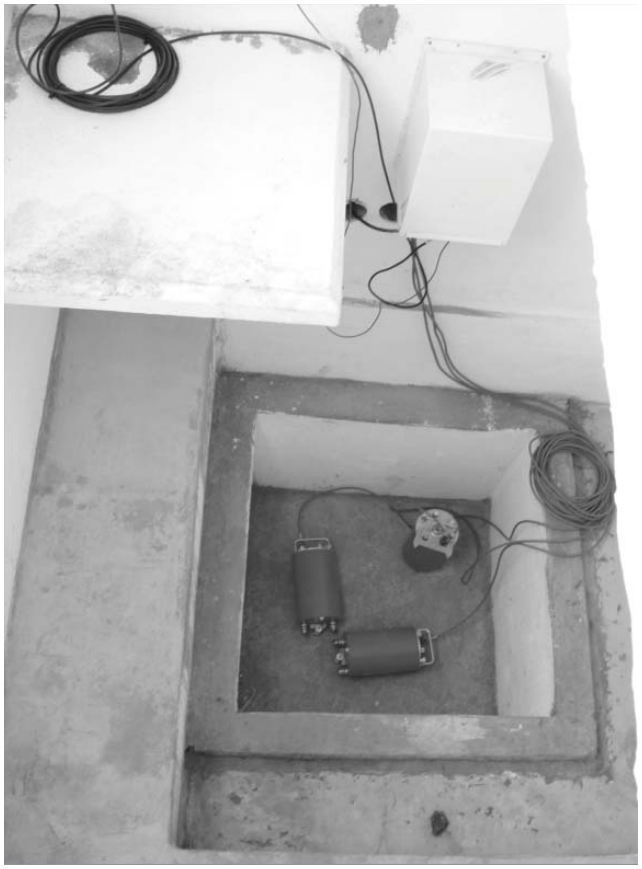

Fig. 3. Picture of the GS-13 short period seismometers at station SPEL (H06S1). This site has one vertical and two horizontal (N-S and E-W) instruments. This is the southern station of the network.

06/10/2004 Kamchatka peninsula.- Due to an error in data handling, only the vertical component at station SPEL is available for this earthquake (M_w=6.8). The epicentral distance is 74.15° (8245 km). Figure 4a shows the detection of both the *P* and *pP* arrivals in the short period record. The spectrogram for this record was calculated using the Seismic Analysis Code (SAC) and is shown in Figure 4b. The *P* arrival has a frequency contents between 0.1 and 3 Hz and reaches a maximum around 1 Hz. The energy for the *pP* wave ranges from 0.1 to 1.5 Hz. The depth of this earthquake (189 km) makes it easier to observe high frequency *P* waves at this distance because the path avoids the high attenuation crust and uppermost mantle on the source side. The great circle path for this event is clear from islands that could block the propagation of the *T* wave (Figure 1), thus making its detection at Socorro Island plausible. Unfortunately data were not available at the expected arrival time.

06/14/2004 Guerrero-Oaxaca border region, Mexico.- This event (M_w=5.9) was recorded at stations SRAD and SPLN. The epicentral distance to SRAD is 12.70° (1413 km). Figure 5a shows the transverse, radial and vertical records from SRAD bandpass filtered between 0.02 and 0.10 Hz (50 to 10 s). The *S* arrival and the surface waves show clearly. The *P* wave shows weakly because the station lies near one of the nodal planes in the focal mechanism obtained from Harvard University's catalog.

06/28 at 05:11 and 18:57 and 06/29/2004 Rivera Fracture Zone (RFZ).- This sequence is made up of three small earthquakes in the Rivera Fracture Zone. The distance from the different events to the stations varies between 209 and 244 km. The coda magnitude for the first event on 6/28 is 4.4, for the second event on the same day it is 3.9 while the event on 6/29 has a magnitude of 4.5. The two events on 6/28 were recorded at all three stations, but the event on 6/29 was not recorded at SRAD because the link with the station broke down starting that day. The hypocenters reported in Table 2 were calculated using the mainland stations of Mexico's Servicio Sismológico Nacional together with all the *P* and *S*

Table 2

List of events recorded on Socorro Island between June 10 and July 9, 2004

Date Y/M/D	Origin time H:M:S	Lat. (°N)	Long (°E)	Depth (km)	Mag.[a]	Distance[b] (km)	No. Stat.[c]	Location	Source[d]
04/06/10	15:19:58	55.68	160.00	189	6.8 M_w	8245	1	Kamchatka peninsula	A
04/06/14	22:54:21	16.34	-97.85	10	5.9 M_w	1420	2	Guerrero-Oaxaca, Mexico	A
04/06/28	05:11:05	19.04	-108.96	5[e]	4.4 M_c	214	3	Rivera Fracture Zone	B
04/06/28	09:49:47	54.80	-134.25	20	6.8 M_w	4453	3	Off the coast of SE Alaska	A
04/06/28	18:57:21	19.11	-108.68	10[e]	3.9 M_c	244	3	Rivera Fracture Zone	B
04/06/29	05:31:14	19.15	-108.91	31	4.5 M_c	221	2	Rivera Fracture Zone	B
04/06/29	07:01:31	10.74	-87.04	9	6.3 M_w	2724	2	Nicaragua-Costa Rica Reg	A
04/07/01[f]	04:39:39	-50.02	162.78	10	6.2 M_w	11333	2	Auckland Islands Region	C
04/07/08	10:30:49	47.22	151.29	133	6.3 M_w	9050	2	Kuril Islands	C
04/07/08	17:33:43	-25.19	-116.17	12	5.6 M_w	4915	2	Southern East Pacific Rise	D
04/07/08	19:54:33	-25.09	-116.00	10	5.9 M_w	4902	2	Southern East Pacific Rise	C
04/07/09f	03:39:31	-26.84	-113.63	10	5.3 M_w	5074	1	Easter Island Region	C

[a]Magnitude: M_w = moment magnitude; M_c = coda magnitude.
[b]Epicentral distance to station SPLN, except for event of 6/10 with a distance to SPEL.
[c]Number of stations available for analysis.
[d]Source of the parameters listed:
A - All parameters from the United States Geological Survey, National Earthquake Information Center as published in the International Seismological Centre's (ISC) web page, except for the magnitude which was taken from the Harvard catalog as published in the ISC's web page.
B - Servicio Sismológico Nacional, using data from the stations on Socorro Island.
C - All parameters from the Preliminary Determination of Epicenters, United States Geological Survey, web page of the National Earthquake Information Center, except for the magnitude which was taken from the Harvard catalog as published in the ISC's web page.
D - All parameters from Harvard's on-line catalog. Time, location and depth are for the centroid.
[e]The depth was constrained to make the location procedure stable.
[f]Data are available from the short period instruments but no seismic or acoustic phases were identified.

picks available from the stations at the island (C. Jiménez, Servicio Sismológico Nacional, personal communication, 2004). These events produced clear surface waves with a dominant period of about 2 s at these distances. The N-S, E-W and vertical components from the first event on 6/28 at station SRAD are shown in Figure 6a. During a temporary deployment at the island in 1999, Valenzuela *et al*. (2005) reported the observation of earthquakes on both the Rivera and Clarión fracture zones.

06/28/2004 Off the coast of southeastern Alaska, United States of America.- This event (M_w=6.8) was recorded by all three stations. The epicentral distance to station SPLN is 40.05° (4453 km). The records clearly show the *P*, *PP*, *S* and *SS* arrivals as well as surface waves. Figure 7 shows the velocity records from station SRAD. Due to an error in data archiving, the records are not long enough to see the arrival of the *T* phase. However, because of the event's location it is not expected that the *T* waves will be recorded as they would be blocked by the west coast of North America (Figure 1).

06/29/2004 Near the coast of Nicaragua-Costa Rica border region.- The earthquake (M_w=6.3) is only observed at stations SPEL and SPLN because station SRAD stopped operating. The epicentral distance to SPLN is 24.50° (2724 km). The *P* arrival and the surface waves were recorded by the short period instruments.

The earthquakes in the Guerrero-Oaxaca border region and off the coast of southeastern Alaska provide examples of the records that can be obtained with the broadband seismometer for moderate to large earthquakes. Under favorable circumstances it is also possible to detect the high frequency *P* waves of teleseismic events, as shown by the intermediate depth earthquake under the Kamchatka Peninsula. The continued operation of the stations on Socorro Island is expected to record earthquakes in the nearby fracture zones (Rivera, Clarión, Orozco, O'Gorman, Clipperton, and Siqueiros FZs). Previous temporary deployments at the island in 1999 (Valenzuela *et al*., 2005) and in 2002 (R. W. Valenzuela, Universidad Nacional Autónoma de México,

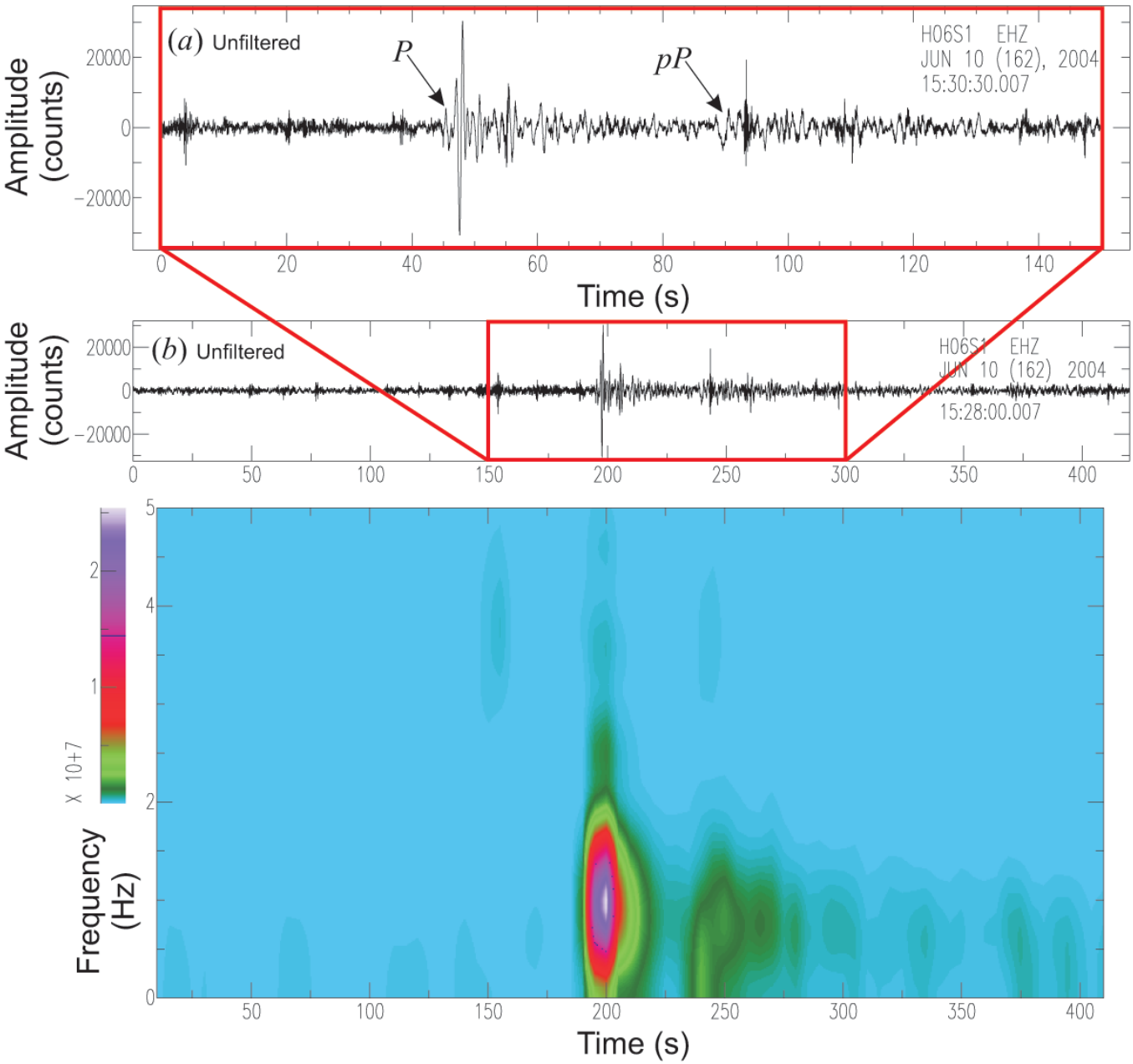

Fig. 4. Vertical component of the unfiltered velocity record for the earthquake in the Kamchatka peninsula, 06/10/2004, at the short period station SPEL (H06S1). (a) the time series shows the high frequency *P* and *pP* arrivals. (b) Spectrogram of the same record. The *P* phase has a frequency contents between 0.1 and 3 Hz, with the maximum around 1 Hz. The energy for the *pP* wave ranges from 0.1 to 1.5 Hz.

unpublished, 2003) recorded events from the Clarión, Rivera and Siqueiros FZs. It is also expected that seismic events associated to the volcanoes on Socorro and San Benedicto islands will be detected should they become active again (Siebe *et al*., 1995; Valenzuela *et al*., 2005).

4. *T* PHASES RECORDED AT SOCORRO ISLAND

In order to extract the time windows containing the *T* phases, the expected travel times were calculated by dividing the epicentral distances listed in Table 2 by 1.484 km/s, the velocity of the *T* wave in the SOFAR channel in the equatorial and tropical Pacific ocean (Johnson and Norris, 1968; Talandier and Okal, 1998). Since the energy of the *T* wave travels at high frequencies, the seismograms were highpass filtered at 1 Hz. Spectrograms were calculated from the filtered records using SAC. *T* phases generated by earthquakes in five different locations around the Pacific were recorded. It is expected that *T* waves from other regions will be detected as more data are collected. When possible, the

calculation of the expected arrival time was improved. A likely point for the conversion of seismic-to-acoustic energy was chosen along the great circle path. The travel time was then determined from the propagation of a seismic wave (either *P* or *S*) through land plus the propagation of an acoustic wave through water (in the SOFAR channel).

T phase observations for the event of 06/14/2004 Guerrero-Oaxaca border region, Mexico.- The *T* phase from this event was recorded at SRAD and SPLN. No record was available from SPEL at the expected arrival time. Figure 5b shows the transverse, radial and vertical records from SRAD highpass filtered at 1 Hz. The *T* phase is clearly visible in all

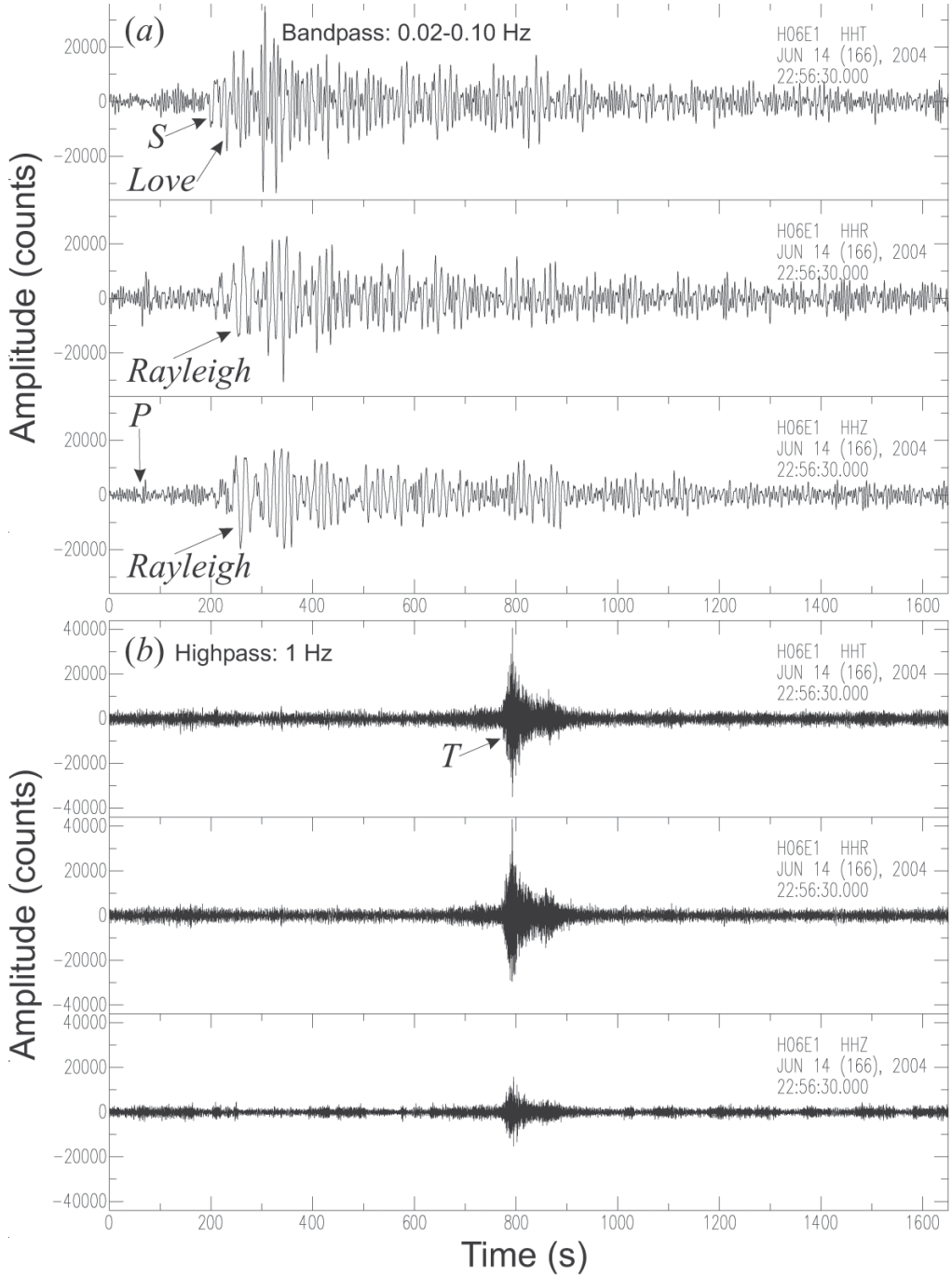

Fig. 5. Velocity records for the earthquake in the Guerrero-Oaxaca border region, 06/14/2004, at the broadband station SRAD (H06E1). The transverse, radial and vertical components are shown. (a) the time series were bandpass filtered between 0.02 and 0.10 Hz. All records are shown at the same scale. Body and surface waves are observed. (b) the records were highpass filtered at 1 Hz in order to show the *T* phase. (c) spectrogram of the filtered transverse component. The early, weak arrival is the $P \rightarrow T$ wave. The second arrival is the $S \rightarrow T$ wave. The third arrival is very clear and it has a predominant frequency around 3.5 Hz. The combined duration for all three arrivals is approximately 200 s.

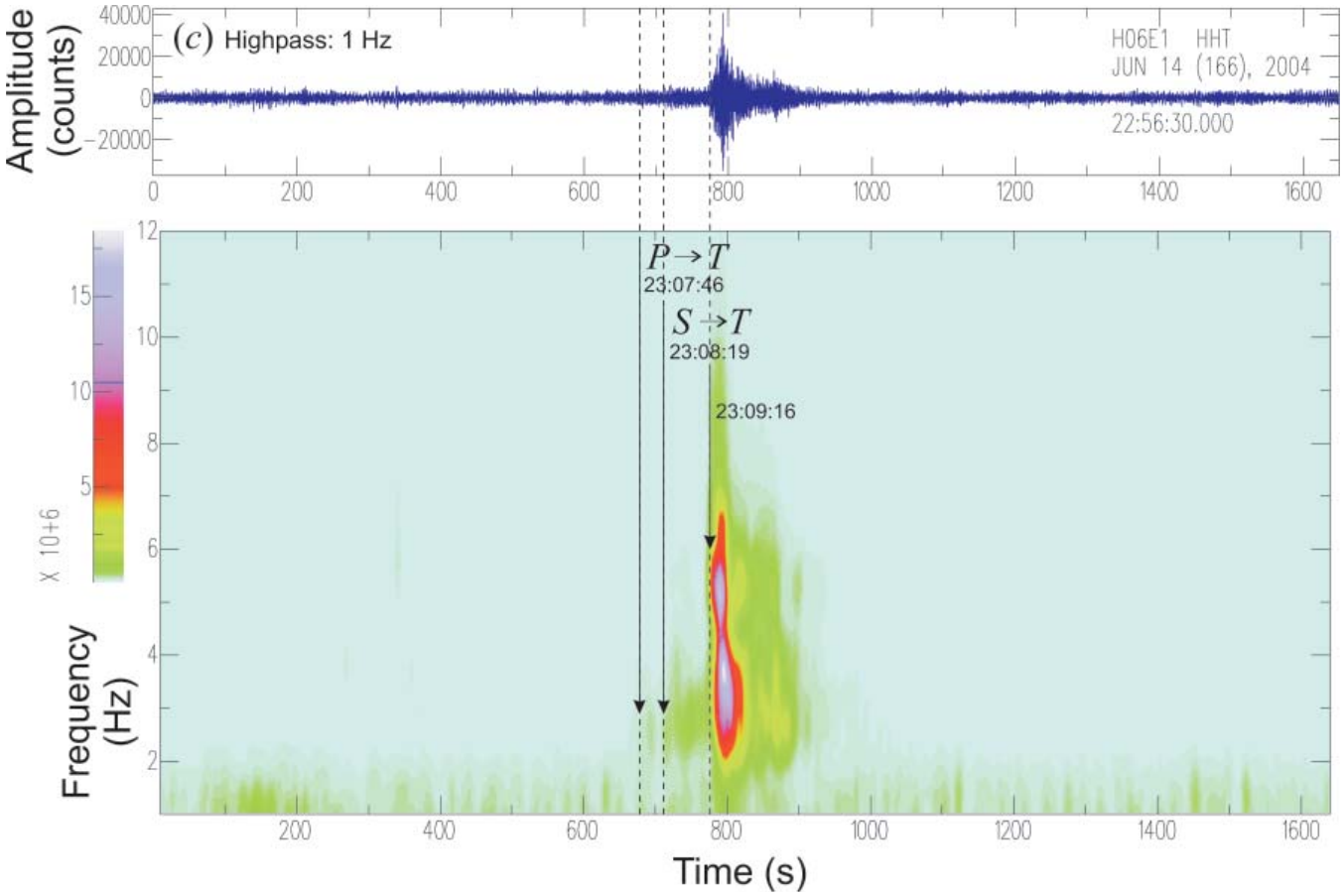

Fig. 5. Continued.

three components. The spectrogram for the highpass filtered transverse component was calculated using SAC, see Figure 5c. The arrival times for the *T* wave were determined from the spectrogram. An early, weak arrival is observed at 23:07:46 ± 5 s, followed by another arrival at 23:08:19 ± 5 s (Figure 5c). A third, very clear arrival is recorded at 23:09:16 ± 5 s. The three arrivals have a combined duration of about 200 s. The energy for the strongest wave has a frequency contents between 1.5 and 11 Hz and reaches its maximum at about 3.5 Hz.

The expected arrival time was calculated assuming that the conversion from seismic to acoustic energy occurs on the continental slope. In this case the great circle path intersects the 1000-m depth contour at a point with the coordinates 16.75°N, 100.30°W (Dirección General de Geografía, 2000). From this point, the distance to the epicenter is 2.38° (or 265 km) and the distance to SRAD is 10.32° (1148 km). The travel time for the *P* wave to the transition point is 39 s, and for the *S* wave it is 69 s. Taking a velocity of 1.484 km/s (Johnson and Norris, 1968; Talandier and Okal, 1998), the acoustic wave has a travel time of 774 s. Therefore, the estimated arrival time is 23:07:54 for the $P \rightarrow T$ wave, and 23:08:24 for the $S \rightarrow T$ wave. The calculated $P \rightarrow T$ arrival is 8 ± 5 s later than the first arrival observed (23:07:46 ± 5 s). The estimated $S \rightarrow T$ arrival time is 5 ± 5 s later than the second arrival recorded (23:08:19 ± 5 s). Given the uncertainty in picking the observed *T* arrival times, and also the uncertainty as to the exact location of the seismic-to-acoustic transition point, the interpretation of the first two arrivals as $P \rightarrow T$ and $S \rightarrow T$ seems appropriate. Valenzuela *et al*. (2005) identified both the $P \rightarrow T$ and $S \rightarrow T$ arrivals from the Tehuacán earthquake of June 15, 1999 (18.15°N, 97.52°W, depth 60 km, M_w=7.0). In that case the energy of the signal was much stronger given the large magnitude of the event. The Tehuacán earthquake was located 205 km north-northeast from the epicenter for the Guerrero-Oaxaca event. The epicentral distance for these two events to station SRAD is similar. It is 1416 km for the Tehuacán earthquake, and 1413 km for the Guerrero-Oaxaca event. The distance between the seismic-to-acoustic transition point and SRAD (directly proportional to the path length through the SOFAR), however, is shorter for the Tehuacán earthquake, only 731 km. In general, the location of these two events and their great circle paths to Socorro Island are similar. Both earthquakes were located in mainland Mexico and their seismic waves traveled west to reach seismic-to-acoustic conversion points at an ocean depth of ~1000 m on the continental slope of the Mexican Pacific ocean. From the conversion points, acoustic waves propagated west to Socorro Island. It is possible that the bathymetry at the seismic-to-

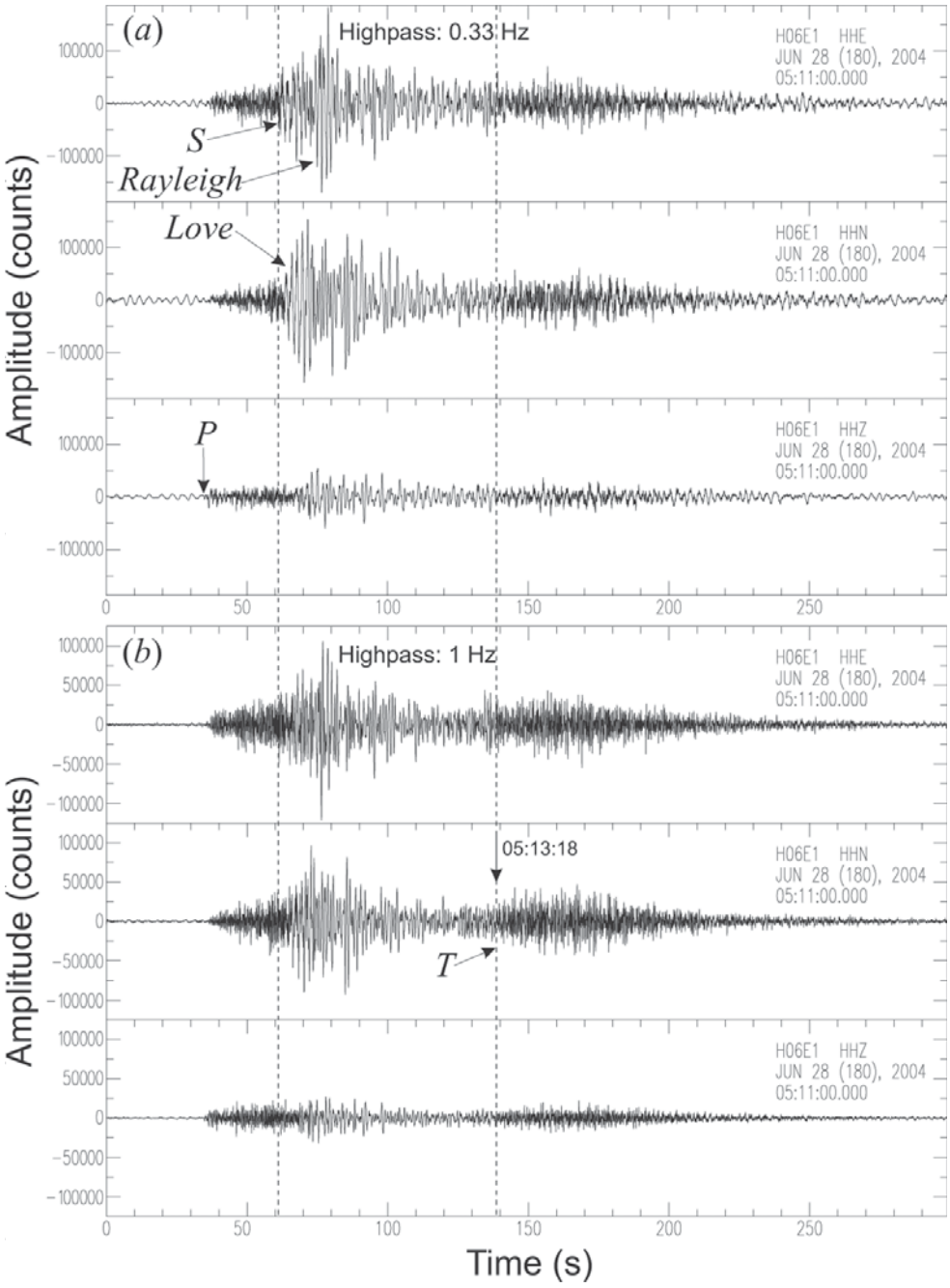

Fig. 6. Velocity records for the Rivera Fracture Zone earthquake, 06/28/2004 at 05:11:05, at the broadband station SRAD (H06E1). The E-W, N-S and vertical components are shown. The station has a backazimuth ϕ_b = 81.9°. (a) the time series were highpass filtered at 0.33 Hz. All records are shown at the same scale. Body, surface and *T* waves are observed. (b) the records were highpass filtered at 1 Hz in order to enhance the T phase. Body and surface waves are still visible. (c) spectrogram of the filtered N-S component. At this distance the surface waves show energy coming in at frequencies starting below 1 Hz and as high as 4 Hz. Energy for the *T* wave is observed at frequencies between 1 and 6 Hz and is strongest between 1.5 and 2.5 Hz. The arrival time of the *T* phase cannot be exactly determined.

acoustic conversion point leads to the efficient generation of $P \rightarrow T$ and $S \rightarrow T$ waves for these paths.

T phase observations for the three events on 06/28 and 29/2004 Rivera Fracture Zone.- As an example, Figure 6b shows the N-S, E-W and vertical components for the first event on 6/28 at SRAD, highpass filtered at 1 Hz. At such a short epicentral distance (1.88° = 209 km) the surface wave train is very close to the arrival of the *T* wave (Figure 6b), thus making it difficult to determine the start time of the *T* phase. It is also difficult to discriminate the surface from the *T* waves because their frequency contents are similar at this distance.

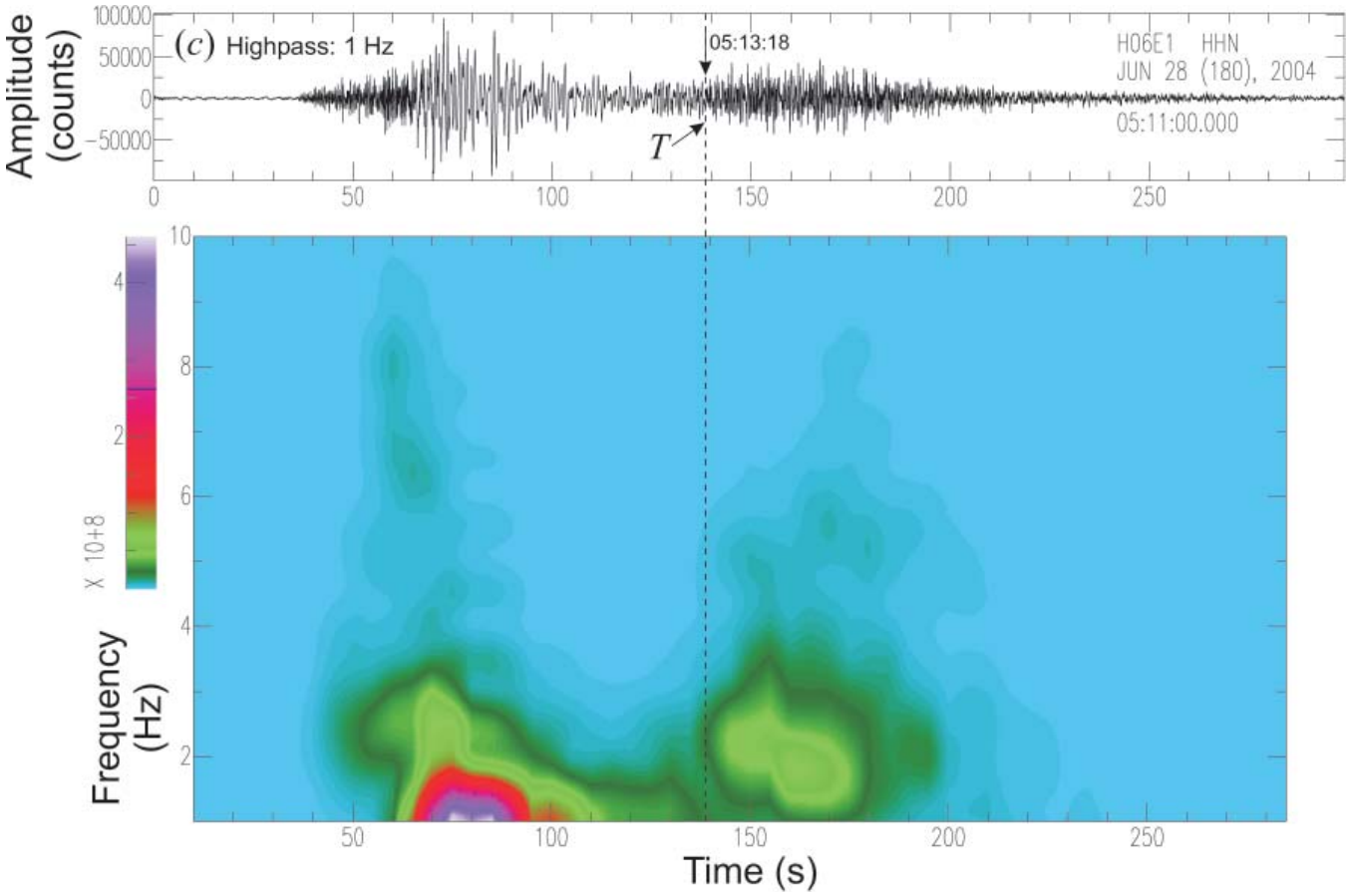

Fig. 6. Continued.

Figure 6c shows the spectrogram for the N-S component. The surface wave energy comes in at frequencies starting below 1 Hz and up to 4 Hz, and is strongest at about 1 Hz (records were highpass filtered at 1 Hz). The energy for the *T* wave arrives at frequencies between 1 and 6 Hz and is strongest between 1.5 and 2.5 Hz. The best estimate for the start time of the *T* phase is at 05:13:18 ± 5 s. This time seems consistent with a calculated "all-oceanic" path (only an acoustic wave traveling through water at the SOFAR velocity) predicting an arrival time at 05:13:26. No bathymetric feature could be identified which would couple the seismic energy to acoustic energy (Dirección General de Geografía, 1988). Perhaps the ridge where the earthquakes occurred serves this function. The ridge's highest elevation is 1967 m below sea level and may, however, be too deep relative to the axis of the SOFAR channel (at about 1000 m below sea level) to efficiently convert seismic energy to acoustic energy. Valenzuela *et al*. (2005) studied the *T* phase from a different, farther earthquake (480 km) also on the Rivera Fracture Zone. They proposed that a seamount would couple the energy into the SOFAR channel. The seamount's highest elevation was 1501 m below sea level and also seems very deep to couple efficiently into the SOFAR channel. An alternative explanation is the detection of the *Ti* phase (Butler and Lomnitz, 2002; Lomnitz *et al*., 2002). This signal propagates along the ocean floor both in the sediments and in the water and travels along a purely oceanic path. *Ti* phases can easily be converted to *P* waves when they encounter an island or a continental shelf (Lomnitz *et al*., 2002). Therefore, *Ti* phases from earthquakes in the Rivera FZ can be recorded at Socorro Island. The *Ti* phase travels at 1.510 km/s, the speed of sound in deep water (Butler and Lomnitz, 2002; Lomnitz *et al*., 2002). This velocity is greater than for waves traveling in the SOFAR, which is a low velocity region. The expected arrival time for the *Ti* phase is at 05:13:23 and is closer to the observed arrival time than the arrival time calculated for propagation through the SOFAR.

T phase observations for the event of 06/29/2004 Near the coast of Nicaragua-Costa Rica border region.- The *T* wave is clearly seen on the records of both SPEL and SPLN, the two stations operating at the time of the event. A spectrogram of the vertical component of SPEL, highpass filtered at 1 Hz, reveals an arrival time for the *T* phase at 07:31:14 ± 5s and a wavetrain approximately 120 s long. The *T* wave energy comes in at frequencies between 1.5 and 8 Hz, with a maximum at about 3 Hz. If the travel time is calculated for a wave propagating entirely through the SOFAR, the expected

arrival time is 07:32:02. The observed early arrival seems to indicate that a portion of the path runs through land. However, it was impossible to ascertain the location of the seismic-to-acoustic transition point. This event occurred very close to the ocean side of the Middle America Trench (Circum-Pacific Map Project, 1977; Dirección General de Geografía, 2000). Therefore, the continental slope is away from Socorro Island, which would actually increase the observed travel time. The arrival time computed for the *Ti* phase (Butler and Lomnitz, 2002; Lomnitz *et al*., 2002) is 07:31:30 and is closer to the observed arrival time than the arrival time calculated for propagation through the SOFAR.

T phase observations for the event of 07/08/2004 Kuril Islands.- The *T* wave is clearly seen in the time domain records at SPLN in the north side of the island. Due to a communication problem with station SPEL in the south, only the vertical component is available. Station SRAD was no longer operating by the time of this earthquake. The velocity records from SPLN were highpass filtered at 1 Hz. Two separate *T* wave packets are observed (Figure 8a). The spectrogram (Figure 8b) for this station shows that the two wave packets are similar in shape and duration although the first one is somewhat more energetic than the second. The first packet arrives at 12:10:17 ± 5 s and lasts for about 100 s. Its frequency contents ranges from about 1.5 to 6 Hz, with a maximum at about 3 Hz. The second packet arrives shortly afterwards at 12:12:11 ± 5 s and also lasts on the order of 100 s. Its energy is contained between 2 and 5.5 Hz, with the maximum at about 3 Hz. Finally, a little more energy is observed after the second packet. The combined duration of all three signals is on the order of 300 s. The highpass filtered vertical velocity record for SPEL in the south side of the island does not show the *T* phase. Calculation of the spectrogram, however, shows the same two main wave packets as the station located in the north of the island. In this case the signal barely stands above the noise produced by the wind. The *T* wave certainly could not be identified from this record alone. Identification is only possible by comparison to the spectrogram from SPLN because the shapes, arrival times and durations of the *T* waves are similar at both stations. The lower signal at the southern station can be explained because the back azimuth for the event is towards the northwest. Consequently, the wave recorded in

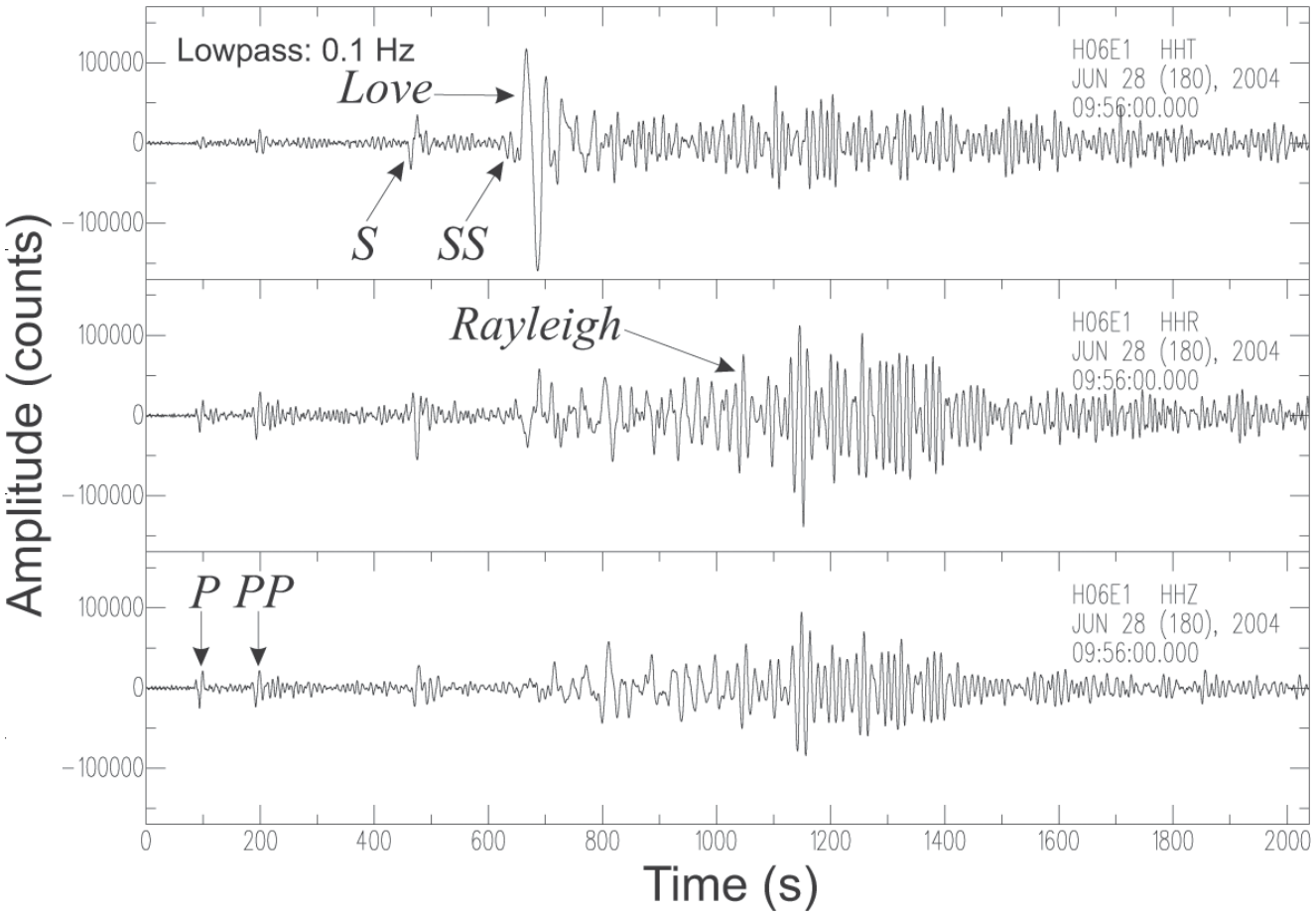

Fig. 7. Velocity records for the earthquake off the coast of southeastern Alaska, 06/28/2004, at the broadband station SRAD (H06E1). The transverse, radial and vertical components are shown. The time series were lowpass filtered at 0.1 Hz in order to remove microseismic noise of period around 3 to 4 s. All records are shown at the same scale. Body and surface waves are observed.

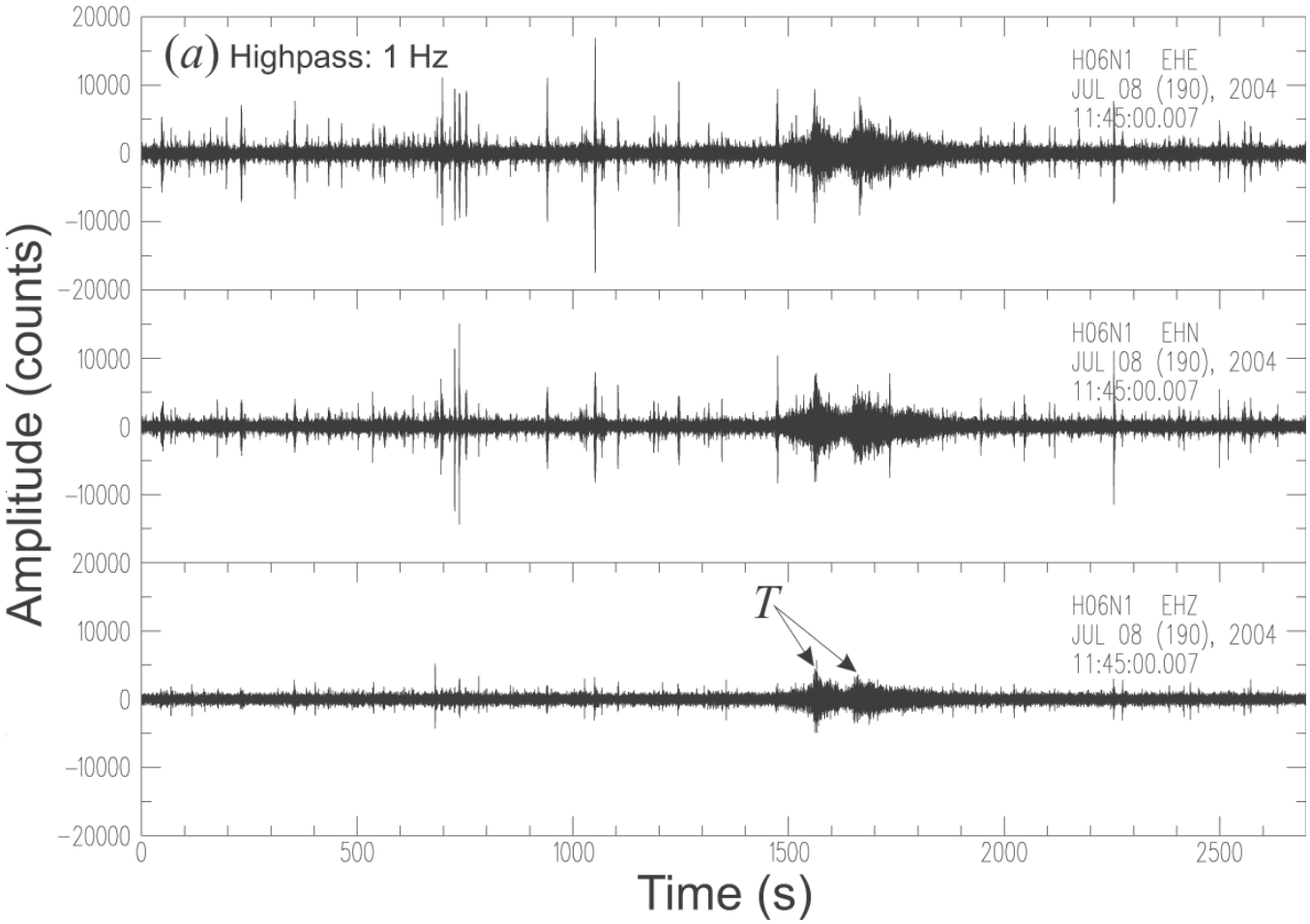

Fig. 8. Velocity records for the earthquake in the Kuril Islands, 07/08/2004, at the short period station SPLN (H06N1). The E-W, N-S and vertical components are shown. (a) the time series were highpass filtered at 1 Hz. All records are shown at the same scale. Two separate *T* arrivals can be seen. The horizontal components are noisier than the vertical. The noise is produced by the wind and has most of its energy at frequencies greater than 8 Hz. (b) spectrogram of the filtered vertical component. The first *T* wave packet has a frequency contents ranging from 1.5 to 6 Hz and its maximum around 3 Hz. The energy for the second wave packet is contained between 2 and 5.5 Hz.

the south has traveled a longer path through the rock of the island and is more attenuated.

The travel time for the *T* wave was calculated from the travel times of a seismic wave propagating through land plus an acoustic wave propagating through water. From a bathymetric map (Circum-Pacific Map Project, 1990), the location on the continental slope of the seismic-to-acoustic transition point was estimated at 48.0°N, 155.0°E. Thus, the distance from the epicenter to the seismic-to-acoustic conversion point is 2.62° (291 km) and the distance from the transition point to SPLN is 78.77° (8759 km). The travel time for the *P* wave to the transition point is 42 s, and for the *S* wave it is 75 s. For an acoustic wave traveling at 1.484 km/s (Johnson and Norris, 1968; Talandier and Okal, 1998), the travel time from the transition point to the station is 5902 s. The expected arrival times at SPLN are 12:09:53 for the $P \rightarrow T$ wave, and 12:10:26 for the $S \rightarrow T$ wave. The calculated arrival time for the $P \rightarrow T$ wave is 24 ± 5 s earlier than the observed arrival (12:10:17 ± 5 s) while the expected $S \rightarrow T$ arrival is 9 ± 5 s later than the recorded arrival. It should be pointed out that the velocity in the SOFAR channel at mid latitudes is lower than near the equator (Johnson and Norris, 1968). Likewise, the depth to the SOFAR is shallower at mid latitudes. The SOFAR velocity around the seismic-to-acoustic conversion point is about 1.454 km/s and the depth to the SOFAR is about 200 m (Johnson and Norris, 1968). Consequently, as the *T* wave travels from the seismic-to-acoustic conversion point to the station (Figure 1), its velocity increases gradually from 1.454 to 1.484 km/s. This means that the expected arrival times actually will be later than those previously calculated at an average velocity of 1.484 km/s. The travel time for the acoustic wave calculated over a distance of 8759 km at a velocity of 1.454 km/s is on the order of 2 minutes longer than if calculated at 1.484 km/s. The agreement between the observed and the calculated arrival times seems reasonable considering that a velocity "somewhat" lower than 1.484 km/s should be used. Furthermore, the uncertainty in reading

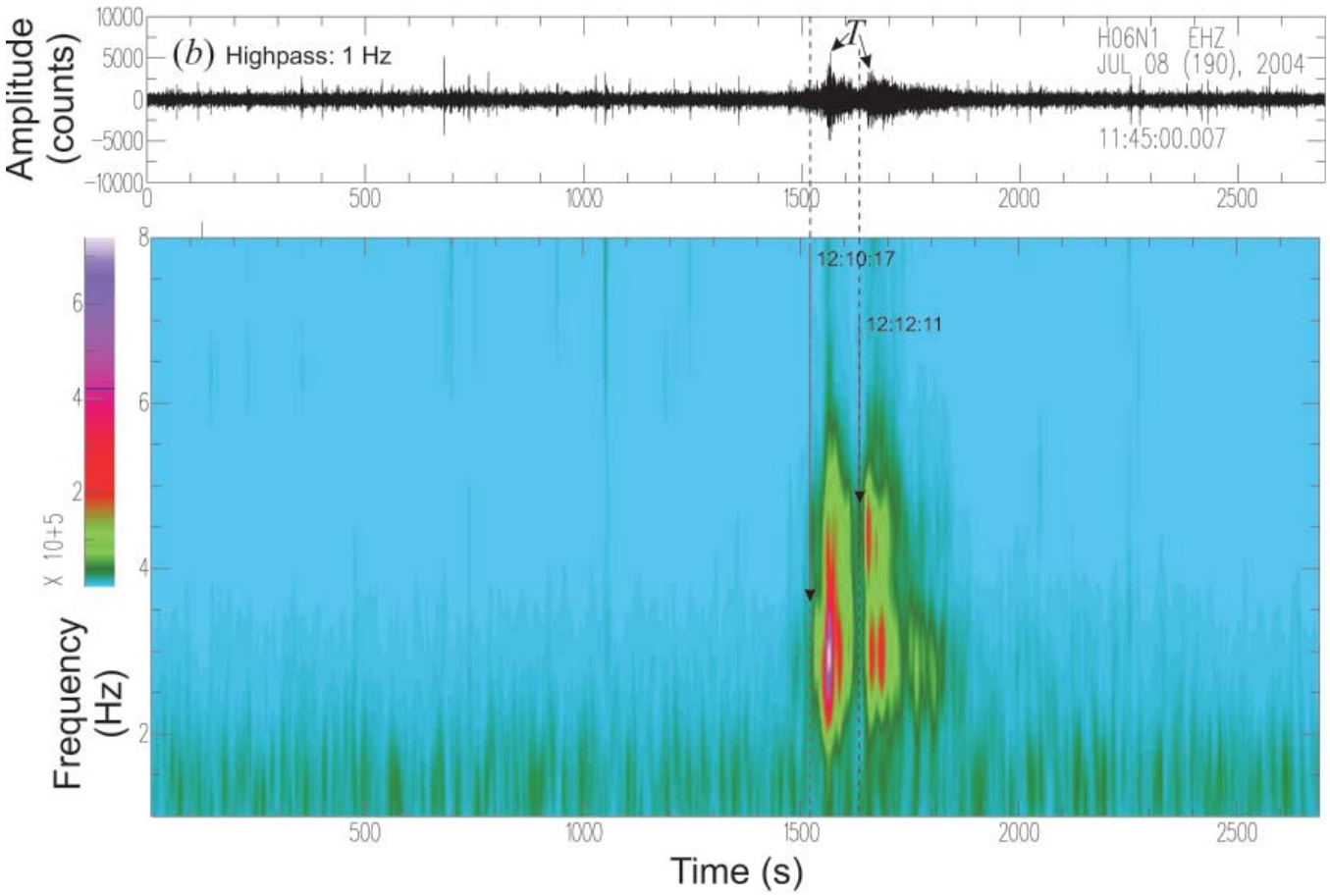

Fig. 8. Continued.

the *T* arrival times and the uncertainty in the location of the transition point also increase the mismatch between observed and calculated values.

T phase observations for the two events on 07/08/2004 Southern East Pacific Rise.- Records are available for these two events only at SPEL and SPLN because SRAD was no longer operational. The second event, at 19:54:33, is the largest (M_w=5.9). The velocity records for this event at SPEL were highpass filtered at 1 Hz and clearly show the *T* phase. Calculation of the spectrogram gives an arrival time at 20:49:13 ± 5 s for a wave packet lasting for approximately 60 s. The frequency contents of the wave goes from 2 to 7.5 Hz, reaching its maximum at about 3.75 Hz. The vertical component at SPLN was bandpass filtered between 2 and 7 Hz in order to get rid of noise from the wind, which is strong at frequencies above 8 Hz. The *T* wave revealed by the spectrogram shows similar characteristics (shape, arrival time and duration) to the one observed in the southern station but is weaker in amplitude. The *T* phase cannot be identified in the spectrograms for the horizontal components from the northern station, possibly because the wind is stronger than in the vertical record, thus resulting in a poorer signal to noise ratio. The back azimuth is towards the south, explaining the better detection of the *T* wave in the southern station.

The epicentral distance to SPEL is 4889 km. Assuming that the whole path were traveled as an acoustic wave at a velocity of 1.484 km/s (Johnson and Norris, 1968; Talandier and Okal, 1998), then the expected *T* arrival time would be 20:49:27. This is 14 ± 5 s later than the observed arrival time (20:49:13 ± 5 s) and may suggest that a portion of the path was traveled as a seismic wave. We looked at a bathymetric map (Circum-Pacific Map Project, 1978) but could not find a suitable seismic-to-acoustic conversion point. The East Pacific Rise runs north of the epicenter, but in this region its highest elevations stand at about 3000 m below sea level, thus making it unlikely that it could couple seismic energy into the SOFAR channel. It should also be noted that further uncertainties in the calculation of the expected arrival time are introduced by the uncertainty of the earthquake location as well as the location of the acoustic-to-seismic transition point. Another possible explanation for the mismatch between the observed and the expected arrival times, as previously suggested for the events in the Rivera Fracture Zone, is the detection of the *Ti* wave at Socorro Island (Lomnitz *et al*.,

2002). However, the *Ti* wave arrival time calculated for a velocity of 1.510 km/s (Butler and Lomnitz, 2002; Lomnitz *et al*., 2002) is 20:48:31, which is 42 ± 5 s earlier than the observed arrival time (20:49:13 ± 5 s).

5. CONCLUSIONS

The seismic and hydroacoustic network installed jointly by the Servicio Sismológico Nacional and the Comprehensive Nuclear-Test-Ban Treaty Organization at Socorro Island started operating in May 2004. Its three stations cover the Pacific ocean in all directions and are used for the detection of *T* waves. We have presented the observations pertaining to ten earthquakes recorded through mid-July of the same year. These events occurred at distances between 209 and 9050 km and ranged in magnitude from 3.9 to 6.8. We recorded one event from the Kamchatka peninsula, one from near the Guerrero-Oaxaca border region, three events in the Rivera Fracture Zone, one off the coast of southeastern Alaska, one near the coast of the Nicaragua-Costa Rica border region, one in the Kuril Islands, and two from the southern East Pacific Rise. The event in the Kamchatka peninsula produced *P* wave energy at short periods at an epicentral distance of 8245 km. These results, together with those from previous temporary deployments, lead to the expectation that many events will be recorded in the fracture zones around the island, especially in the Rivera Fracture Zone. It should also be possible to monitor the seismic activity associated with volcanic events in Socorro and San Benedicto Islands.

T waves produced by earthquakes in five different locations around the Pacific ocean were recorded. In a few cases, such as for large or nearby events, it was possible to detect *T* phases in both the near and the far sides of the island relative to the epicenter. For small or distant sources it was difficult, some times impossible, to identify the *T* wave in the far side of the island. These observations validate the approach of deploying three stations around the island. For events such as the one in the Guerrero-Oaxaca border region and the one in the Kuril Islands it was possible to locate the seismic-to-acoustic conversion point on the continental slope from bathymetry data. However, this determination was not possible for the event near the coast of the Nicaragua-Costa Rica border region. The clusters of events in both the Rivera Fracture Zone and the Southern East Pacific Rise could not be associated with specific transition points, but have *T* wave travel times suggesting that most of their path is through the SOFAR channel, with very short segments of propagation as a seismic wave. Therefore the question as to how some *T* phases are generated still remains open and may prove an interesting area for further research.

ACKNOWLEDGMENTS

We thank the Mexican Navy, the Ministry of Foreign Affairs, the Ministry of Energy, the Ministry of the Interior, the Ministry for the Environment and Natural Resources, and the Ministry for Communications and Transportation of the Mexican government for their valuable assistance making this work possible. We thank Captain Mariano Barrón Mares for his help in Manzanillo in order to carry out the construction at the island. We are grateful to the late Cecilio Rebollar and to two anonymous reviewers for discussions and suggestions. We thank Shri Krishna Singh for his guidance while working on this project. We thank Casiano Jiménez for relocating the Rivera Fracture Zone events using SSN data including the stations on Socorro Island. We are thankful to Osvaldo Sánchez Zamora for help with preparations for this project; Enedina Martínez, Patricia Medina, and Adriana López for help with the paperwork for permitting and building the network; and Martín Malagón for driving equipment and materials to Manzanillo.

BIBLIOGRAPHY

BUTLER, R. and C. LOMNITZ, 2002. Coupled seismoacoustic modes on the seafloor. *Geophys. Res. Lett., 29*, doi:10.1029/2002GL014722.

CIRCUM-PACIFIC MAP PROJECT, 1977. Geographic map of the Circum-Pacific region: Northeast quadrant, scale 1:10,000,000, Circum-Pacific Council for Energy and Mineral Resources, American Association of Petroleum Geologists, Tulsa, Oklahoma.

CIRCUM-PACIFIC MAP PROJECT, 1978. Geographic map of the Circum-Pacific region: Southeast quadrant, scale 1:10,000,000, Circum-Pacific Council for Energy and Mineral Resources, American Association of Petroleum Geologists, Tulsa, Oklahoma.

CIRCUM-PACIFIC MAP PROJECT, 1990. Geographic map of the Circum-Pacific region: Arctic sheet, scale 1:10,000,000, Circum-Pacific Council for Energy and Mineral Resources, American Association of Petroleum Geologists, Tulsa, Oklahoma.

DIRECCIÓN GENERAL DE GEOGRAFÍA, 1988. Islas Revillagigedo, Map CB-006, First edition, Second printing, scale 1:1,000,000, Instituto Nacional de Estadística, Geografía e Informática (INEGI), Mexico City, Mexico.

DIRECCIÓN GENERAL DE GEOGRAFÍA, 2000. Estados Unidos Mexicanos, Carta hipsográfica en relieve, Second edition, First printing, scale 1:4,000,000, Instituto Nacional de Estadística, Geografía e Informática (INEGI), Aguascalientes City, Mexico.

JOHNSON, R. H. and R. A. NORRIS, 1968. Geographic variation of Sofar speed and axis depth in the Pacific Ocean. *J. Geophys. Res., 73*, 4695-4700.

LOMNITZ, C., R. BUTLER and O. NOVARO, 2002. Coupled modes at interfaces: A review. *Geofísica Internacional, 41*, 77-86.

NEWTON, J. and M. GALINDO, 2001. Hydroacoustic Monitoring Network. Sea Technology, September, 41-47.

OKAL, E. A., 2001. *T*-phase stations for the International Monitoring System of the Comprehensive Nuclear-Test Ban Treaty: A global perspective. *Seism. Res. Lett., 72*, 186-196.

SIEBE, C., J.-C. KOMOROWSKI, C. NAVARRO, J. McHONE, H. DELGADO and A. CORTÉS, 1995. Submarine eruption near Socorro Island, Mexico: Geochemistry and scanning electron microscopy studies of floating scoria and reticulite. *J. Volcanol. and Geothermal Res., 68*, 239-271.

SULLIVAN, J. D., 1998. The Comprehensive Test Ban Treaty. *Physics Today, 51, 3*, 24-29.

TALANDIER, J. and E. A. OKAL, 1998. On the mechanism of conversion of seismic waves to and from *T* waves in the vicinity of island shores. *Bull. Seism. Soc. Am., 88*, 621-632.

VALENZUELA, R. W., M. GALINDO, J. F. PACHECO, A. IGLESIAS, L. F. TERAN, J. L. BARREDA and C. COBA, 2005. Seismic survey in southeastern Socorro Island: Background noise measurements, seismic events and *T* phases. *Geofísica Internacional, 44,* 23-38.

Raúl W. Valenzuela[1], Javier F. Pacheco[1], José Pereira[2], Jorge A. Estrada[3], Jesús A. Pérez[3], José L. Cruz[3], Dario Baturan[4], Arturo Cárdenas[3] and José A. Santiago[3]

[1] *Departamento de Sismología, Instituto de Geofísica, Universidad Nacional Autónoma de México, Circuito de la Investigación S/N, Cd. Universitaria, Del. Coyoacán, México, D. F., C. P. 04510. México,*
Email: raul@ollin.igeofcu.unam.mx

[2] *Hydroacoustic Monitoring Section, International Monitoring System Division, Comprehensive Nuclear-Test-Ban Treaty Organization, Vienna International Centre, P. O. Box 1250, A-1400 Vienna, Austria.*

[3] *Servicio Sismológico Nacional, Instituto de Geofísica, Universidad Nacional Autónoma de México, Circuito de la Investigación S/N, Cd. Universitaria, Del. Coyoacán, México, D. F., C. P. 04510. México.*

[4] *Nanometrics, Inc., 250 Herzberg Rd., Kanata, Ontario, K2K 2A1, Canada*